

*Original Research Article*

# Synergistic Effect of Chitosan on the Antibacterial Properties of Polyvinylidene Fluoride (PVDF) Membranes

Kuganagiesry Subramaniam<sup>1</sup>, Ain Nur Nadhira Shurizan<sup>1</sup>, Nur Suhaili Mohd Yatim<sup>1,2\*</sup>

<sup>1</sup>Faculty of Chemical Engineering & Technology, Universiti Malaysia Perlis, Perlis, 02600 Arau, Malaysia

<sup>2</sup>Centre of Excellence for Biomass Utilization (CoEBU), Universiti Malaysia Perlis (UniMAP), Kompleks Pusat Pengajian Jejawi 3, 02600 Arau, Perlis, Malaysia

[irashurizan@gmail.com](mailto:irashurizan@gmail.com)

\*Corresponding author: Faculty of Chemical Engineering & Technology, Universiti Malaysia Perlis, Perlis, 02600 Arau, Malaysia; [nursuhaili@unimap.edu.my](mailto:nursuhaili@unimap.edu.my)

**Abstract:** Phase inversion is a mixing process where an initially homogeneous polymer solution is controlled to transform from a liquid to a solid phase. This approach has been widely employed in various sectors, including wastewater treatment. However, the use of membrane technology in high-concentration wastewater can lead to pore wetting and clogging due to the accumulation of large foreign particles, resulting in bacterial growth and pollution. To address this issue, the membrane must have a low value of water contact angle, a high percentage of porosity, and must have a great antibacterial property. In this study, it is observed that the addition of chitosan to the polyvinylidene fluoride (PVDF) matrix has improved the water resistance of the membrane, resulting in a decreased value of contact angle. Nevertheless, the 2.0 g chitosan/PVDF membrane is more practical to be used in the wastewater treatment industry compared to the pure PVDF membrane. This is because the chitosan/PVDF membrane has the highest percentage of porosity and the lowest value of water contact angle, which causes the membrane to be less prone to wetting and acts as an excellent barrier against bacterial contamination compared to the other membranes.

**Keywords:** PVDF membrane; Chitosan; Antibacterial

**Received:** 28<sup>th</sup> December 2024

**Accepted:** 22<sup>nd</sup> December 2025

**Available Online:** 30<sup>th</sup> March 2026

**Published:** 30<sup>th</sup> June 2026

**Citation:** Subramaniam, K., Shurizan, A. N. N., & Mohd Yatim, N. S. Synergistic effect of chitosan on the antibacterial properties of poly (Vinylidene Fluoride) (PVDF) Membranes. *Adv Agri Food Res J* 2026; 7(1): a0000571. <https://doi.org/10.36877/aafrij.a0000571>

## 1. Introduction

In industrial wastewater treatment, polymeric membranes are favoured over inorganic membranes due to their greater flexibility, ease of usage, and lower cost. High chemical stability, hydrophobicity, porosity, and suitable stability of polymeric membranes are the

primary attributes that make them suitable for wastewater treatment. Polyvinylidene fluoride (PVDF) is one of the polymers utilised in polymeric membranes because of its exceptional mechanical strength, oxidation resistance, thermal stability, chemical resistance, and hydrophobicity. Nevertheless, the use of polymers in filtration has significant disadvantages, such as membrane fouling and hydrophobic properties. Since PVDF membranes are hydrophobic, their uses are limited due to fouling during separation processes, which results in low flux, short service life, high operating costs, and reduced membrane efficiency. Chitosan is a very cost-effective, non-hazardous, antibacterial substance formed by alkaline N-deacetylation of chitin. Because of its many beneficial qualities, including its ability to be hydrophilic, biodegradable, antibacterial, and antifouling, chitosan is highly appealing (Kumari & Kishor, 2020). Compared to previous studies, most researchers used Titanium Oxide (TiO<sub>2</sub>) to enhance the antibacterial properties of the PVDF membranes. In this study, chitosan is utilised as an agent that can provide antibacterial protection for PVDF membranes. Although chitosan is a very beneficial addition to the PVDF membrane, it may also reduce the membrane's roughness, which would lower the contact angle. Because chitosan is hydrophilic, the membrane is more likely to get wet, which reduces its use in the wastewater treatment industry (Kumari & Kishor, 2020). This research aims to study the effect of different chitosan concentrations on the characteristics and antibacterial properties of the PVDF membranes. Lastly, this study can help to solve contemporary water pollution challenges, which contribute to the achievement of the “Clean Water and Sanitation” of the 17 Sustainable Development Goals (SDGs).

## **2. Materials and Methods**

### *2.1. Preparation of Chitosan*

The ultrasonication method was utilised to dissolve 0.1 g of chitosan in 100 mL of distilled water for 10 min. The dispersed material was transferred to a centrifuge tube and centrifuged for 10 min at a speed of 5000 rpm. After removing the supernatant from the centrifuge tube, the chitosan precipitate was dried for 24 h at 70°C in an oven. After 24 h, the precipitate was cooled to room temperature for 1 h. The mortar and pestle were used to grind the dried product into fine powder. The above steps were repeated two times using 1.0 g and 2.0 g of chitosan.

### *2.2. Preparation of Pure PVDF Membrane*

To eliminate moisture, the PVDF powder was dried in an oven for 24 h at a temperature of 80°C. Then, in a sealed glass flask, 20 g of PVDF was dissolved in 100 mL

of N-methyl-2-pyrrolidinone (NMP) and stirred constantly. For 24 h, the solution was agitated at 250 rpm at 40°C. After the homogenous mixture forms, the solution was kept in a desiccator.

### *2.3. Preparation of Chitosan/PVDF Membrane*

The PVDF powder was dried in the oven for 24 h at 80°C to remove moisture. Then, 20 g of PVDF was dissolved in 100 mL of N-methyl-2-pyrrolidinone (NMP). The mixture was then mixed with the prepared 0.1 g of chitosan and agitated in a sealed glass beaker. Next, the solution was stirred at 250 rpm at a temperature of 40°C for 24 h. After the homogenous mixture formed, the solution was kept in a desiccator. The above steps were repeated two times using 1.0 g and 2.0 g of the prepared chitosan.

### *2.4. Casting of Membranes*

Firstly, the pure PVDF solution was poured into a casting knife, which was placed on a glass sheet. Before casting the membrane, the casting knife was placed at the right position, which shows the 200 µm thickness of the membrane. After that, the glass sheet was immersed in isopropanol (IPA) for 2 sec and then immersed in water immediately at room temperature for 24 h for precipitation to occur. Then, the membrane on the glass sheet was allowed to dry for 1 to 2 days. Thereafter, the membrane was peeled off the glass sheet, washed, and stored. The steps were repeated using 0.1 g, 1.0 g, and 2.0 g of the prepared chitosan.

### *2.5. Water Contact Angle Measurement*

A sessile drop method was used to measure the water contact angle on the membrane's surface. A drop of distilled water at ambient temperature was put onto the pure PVDF membrane using a dropper. Then, the close-up image of the water drop was manually captured using a cell phone's camera. A cell phone's camera was utilised because there was no optical tensiometer available. After capturing the image, the Image J software was used to measure the contact angle of the water droplet. The above steps were repeated three times using 0.1 g, 1.0 g, and 2.0 g chitosan/PVDF membranes. The results obtained were observed and recorded.

### *2.6. Membrane Porosity*

The porosity of the membranes was calculated using the gravimetric method. The membranes of each type were weighed using an analytical balance. The weighed membranes

were immersed in n-butanol for 2 h. Then, the sample is taken out from immersion and blotted till dry using a filter paper and weighed. The membranes were then dried in an oven to remove moisture. The dry membranes were weighed, and the data obtained were recorded. The data was inserted into the porosity equation as stated in Equation 1 below:

$$\text{Porosity } (\varepsilon) = \frac{w_2 - w_1}{A \times t \times \rho} \times 100\% \quad (1)$$

$w_1$  is the weight of the dry sample.

$w_2$  is the weight of the wet sample.

$A$  is the cross-sectional area of the sample.

$t$  is the thickness of the sample.

$\rho$  is the density of the sample.

### 2.7. Scanning Electron Microscopy (SEM) Analysis

The surface morphology and microstructure of the pure PVDF, 0.1 g, 1.0 g, and 2.0 g chitosan/PVDF membranes were analysed using a scanning electron microscope. After the analysis, the samples of the membranes were cut into 1 cm × 1 cm squares and covered with a thin coating of platinum to prevent electric charge. An accelerating voltage of 15 kV was supplied through a high vacuum to generate a beam of electrons, which was used to study the surface morphologies of chitosan. To provide clear pictures, micrographs were taken at 1000× magnification (Ali, *et al.*, 2023).

### 2.8. Fourier-Transform Infrared Spectroscopy (FTIR) Analysis

The functional groups and chemical bonds or structures of the membranes can be determined from the FTIR analysis (Pasiczna-Patkowska *et al.*, 2025) by generating an infrared absorption spectrum of PVDF and chitosan. The pure PVDF, 0.1 g, 1.0 g, and 2.0g chitosan/PVDF membranes were placed under the scope of the FTIR equipment. A spectrum of 4000 to 400 cm<sup>-1</sup> in the mid-infrared region (IR) range with a resolution of 1 cm<sup>-1</sup> was collected. The data obtained were compared.

### 2.9. Halo Zone Test (Kirby–Bauer Test)

Firstly, a nutrient agar and a nutrient broth must be prepared. Nutrient agar is a substance that solidifies and gives organisms a secure surface to develop on. Nutrient broth usually consists of peptone, yeast extract, sodium chloride, and glucose for the microorganisms to feed on. 1.3 g of nutrient broth was dissolved in 100 mL of distilled water in a Scott bottle. In another bottle, 2.3 g of nutrient agar was dissolved in 100 mL of distilled water. Both bottles were loosely capped and autoclaved at 120°C for 1 h. The bottle was then

allowed to cool down to about 48°C to 50°C. Then, *Escherichia. Coli* was used and cultivated in the cooled nutrient broth mixture and placed in an incubator at 37°C for 24 h. As for the nutrient agar mixture, it was poured into 4 different Petri dishes and allowed to harden before being sealed and placed in the refrigerator. After 24 h, a laminar flow cabinet was UV sterilised for 15 min before transferring *E. coli* into the petri dish to avoid contamination. A small piece of the pure PVDF membrane was cut using scissors and placed on a petri dish that contained the solidified nutrient agar. After that, 100 µL of the *E. coli* broth culture was inserted into the dish. The petri dish was sealed and incubated at 37°C for 24 h. The steps were repeated 3 times using the 0.1 g, 1.0 g, and 2.0 g chitosan/PVDF membranes. The inhibition zone for each membrane was observed and recorded.

### 3. Results and Discussions

#### 3.1. Characterisation of Membrane

##### 3.1.1. Water contact angle measurement

The water contact angle measurement was measured and recorded by manually capturing the image of a water droplet on the sample using a camera and processing the image in ImageJ software of the pure PVDF, 0.1g, 1.0g, and 2.0g chitosan/PVDF membranes. Table 1 below provides a summary of the water contact angle data for each of the membranes.

**Table 1.** Contact angle of membranes

Type of membranes	Contact angle
Pure PVDF	101.30°
0.1g chitosan/PVDF	92.52°
1.0g chitosan/PVDF	70.35°
2.0g chitosan/PVDF	66.46°

Hydrophobic materials have a wide contact angle of 90° or greater, while hydrophilic materials have values less than 90° (Abriyanto, 2021). From Table 1, the pure PVDF membrane had the highest water contact angle, while the 2.0 g chitosan/PVDF had the lowest water contact angle. Strong adhesion-adsorption forces make PVDF polymer extremely prone to fouling from foulant interactions with the membrane surface and almost no hydrogen bonding interactions in the water-membrane interface boundary layer. As a result of the random phenomenon of water molecules moving away from the hydrophobic membrane surface, foulant molecules start to adsorb to the membrane's surface, controlling the boundary

layer and the concentration polarisation process that takes place during the filtration process (Abriyanto, 2021).

For the chitosan/PVDF membranes, it can be observed that the 0.1 g chitosan/PVDF membrane had the highest value of water contact angle, followed by 1.0 g and 2.0 g chitosan/PVDF membranes. Despite the addition of 0.1 g of chitosan, the PVDF membrane still exhibited hydrophobic properties. This shows that the small addition of chitosan to the PVDF membrane does not show any significant difference. However, the water contact angles of the 1.0 g and 2.0 g chitosan/PVDF membranes were less than  $90^\circ$ . This is due to the accumulation of hydrophilic chitosan particles on the membrane's surface and perhaps within its pores (Xie, *et al.*, 2018). In addition, hydrophilic membranes with high surface tension can create hydrogen bonds with nearby water molecules to restore the thin water barrier between the membrane and the condensed liquid. This layer prevents or reduces impurities that adhere to the membrane's surface (Abriyanto, 2021). In conclusion, the 2.0 g chitosan/PVDF shows that it is resistant to fouling and able to prevent microbial adhesion.

### 3.1.2. Scanning Electron Microscopy (SEM)

The pure PVDF, 0.1 g, 1.0 g, and 2.0 g chitosan/PVDF membranes were displayed under 1000x magnification. Figure 1 shows the SEM images of the pure PVDF, 0.1 g, 1.0 g, and 2.0 g chitosan/PVDF membranes.

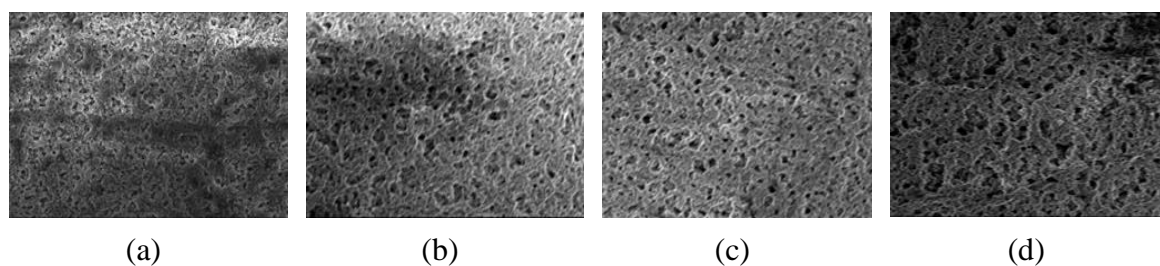


**Figure 1.** SEM images for (a) pure PVDF, (b) 0.1 g chitosan/PVDF, (c) 1.0 g chitosan/PVDF, and (d) 2.0 g chitosan/PVDF membranes

Every membrane has a permeable structure. All membrane types have a fibrous structure that is interconnected and shows slight changes in overall appearance. From this analysis, the pore size of each membrane can be observed and compared. The pure PVDF membrane has a lot of small pores, and its pore size is the smallest compared to the chitosan/PVDF membranes. This dense structure causes the membrane to exhibit hydrophobic properties.

For the chitosan/PVDF membranes, it can be observed that the pore size of the 0.1 g chitosan/PVDF membrane was the smallest but larger than the pore size of the pure PVDF membrane, followed by the pore size of the 1.0 g and 2.0 g chitosan/PVDF membranes. Takeaway from this, the pore size of the membrane becomes larger when the concentration of the chitosan increases. The addition of the chitosan causes the pore size to become larger, and the membrane has a more open structure. This morphological change may be explained by the fact that when the concentration of hydrophilic chitosan particles increases, more non-solvent (water) enters the cast film, and as a result, it creates larger pores. Additionally, the addition of chitosan to PVDF membranes alters the membrane formation process, which can result in decreased pore sizes due to modifications in phase separation kinetics and pore structure development (De Santa Catarina *et al.*, 2022). As a conclusion, the higher the concentration of chitosan blended with the PVDF polymer, the pore size of the membrane becomes larger, resulting in a more porous membrane.

### 3.1.3. Membrane porosity

The porosity of a membrane, defined as the volume fraction of void space within its structure, significantly influences its wettability, which is the tendency of a liquid to spread and adhere to its surface. This study compared the porosity of pure PVDF, 0.1 g, 1.0 g, and 2.0 g chitosan/PVDF membranes. Table 2 below shows the data on the porosity of the membranes.

**Table 2.** Simplified data of porosity percentage

Type of Membranes	Porosity (%)
Pure PVDF	27.7
0.1 g chitosan/PVDF	29.73
1.0 g chitosan/PVDF	37.22
2.0 g chitosan/PVDF	41.54

A higher porosity percentage allows liquids to penetrate the membrane structure promoting surface wetting. The porosity of a membrane correlates with its pore sizes. From Table 2, it can be observed that the pure PVDF has the lowest percentage of porosity compared to the chitosan/PVDF membranes. This is because the membrane has a lot of small pores and a dense membrane structure. When the membrane has a dense structure, it is almost impossible for a liquid to pass through the membrane. This causes the pure PVDF to have a hydrophobic property.

For the chitosan/PVDF membranes, the 2.0 g chitosan/PVDF membrane has the highest percentage of porosity compared to the 0.1 g and 1.0 g chitosan/PVDF membranes. This is because the pore size of the 2.0 g chitosan/PVDF membrane is the largest, and the structure of the membrane is more porous. This results from a repulsive force that was created in the casting solution between the hydrophilic and hydrophobic properties of the chitosan and PVDF. The shrinkage of the organic phase during the blending process creates interfacial pores, which are induced by the strong interfacial bond that forms between the PVDF and chitosan (Purkait *et al.*, 2018). When it comes to chitosan membranes, a clearly defined porous structure can offer improved permeability and adsorption of impurities. This is because the porous structures' mass transfer resistances decrease, so their capacity for void adsorption increases, and their water absorption property also increases. Knowing that hydrophilic chitosan molecules are drawn to water, the water-to-polymer concentration ratio rises as well.

#### 3.1.4. FTIR analysis

The functional group and chemical bonding of the Pure PVDF, 0.1g chitosan/PVDF, 1.0g chitosan/PVDF, and 2.0g chitosan/PVDF membranes were studied using their FTIR spectra, which are displayed in Figure 2. Table 3 shows the wavelengths and functional groups in the pure PVDF, 0.1 g chitosan/PVDF, 1.0 g chitosan/PVDF, and 2.0 g chitosan/PVDF membranes.

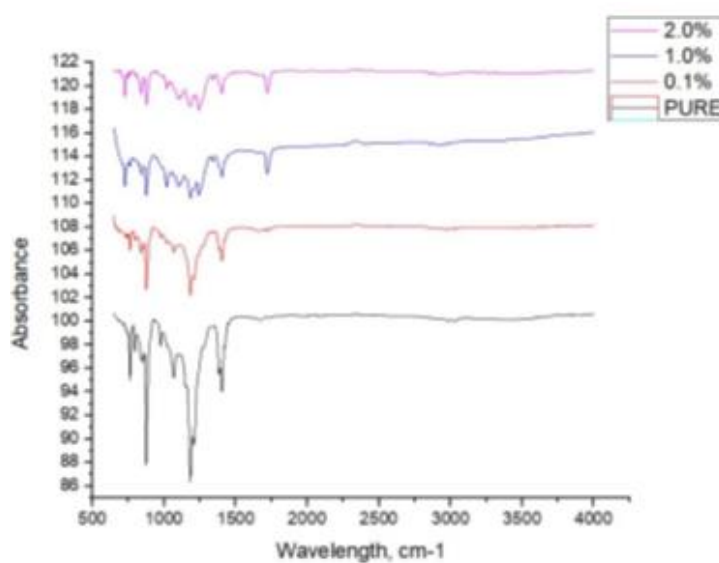


**Figure 2.** FTIR spectra of pure PVDF, 0.1g chitosan/PVDF, 1.0g chitosan/PVDF and 2.0g chitosan/PVDF membranes.

**Table 3.** Wavelengths and functional groups of pure PVDF, 0.1 g chitosan/PVDF, 1.0 g chitosan/PVDF, and 2.0 g chitosan/PVDF membranes.

Types of membranes	Wavelengths (cm <sup>-1</sup> )	Functional groups
Pure PVDF	762	C – H
	874	C – H
	1183	C – F
	1404	C – H
0.1 g chitosan/PVDF	761.64	C – H
	875	C – H
	1182	C – F
	1404	O – H
	1017	C – F
1.0 g chitosan/PVDF	1183	C – F
	1245	C – O
	1405	O – H
	1717	C = O
2.0 g chitosan/PVDF	1180	C – F
	1245	C – O
	1406	O – H
	1718	C = O

Certain chemical bond vibration patterns correlate with wavelengths in the infrared spectrum. Stronger bonds are formed because the wavelength and atomic vibration energy are inversely related. The junction between the incident beam frequency and the bond's vibrational frequency results in infrared absorption. This condition creates peaks that make it possible to identify their functional group (Jiang *et al.*, 2023). According to the results, the pure PVDF membrane is made up of more functional groups that have wavelengths between 1404 and 1183 cm<sup>-1</sup>. PVDF's FTIR spectra display peaks associated with the carbon-hydrogen bending vibration (C – H), and C – F stretching vibration. The C – F functional group indicates that the membrane contains mostly fluoro compounds.

For the chitosan/PVDF membranes, all the chitosan/PVDF membranes have O – H functional groups. This proved that the membranes contain chitosan particles. This is because chitosan contains an O – H functional group in its structure. Other than that, there is also a presence of the C – F functional group in its structure.

### 3.1.5. Antimicrobial-test (Kirby-Bauer/ Halo-zone test)

The resistance of pure PVDF, 0.1 g, 1.0 g, and 2.0 g chitosan/PVDF membranes to bacterial contamination was evaluated after 24 h of incubation period at 37°C. The results are displayed in Figure 3 below.

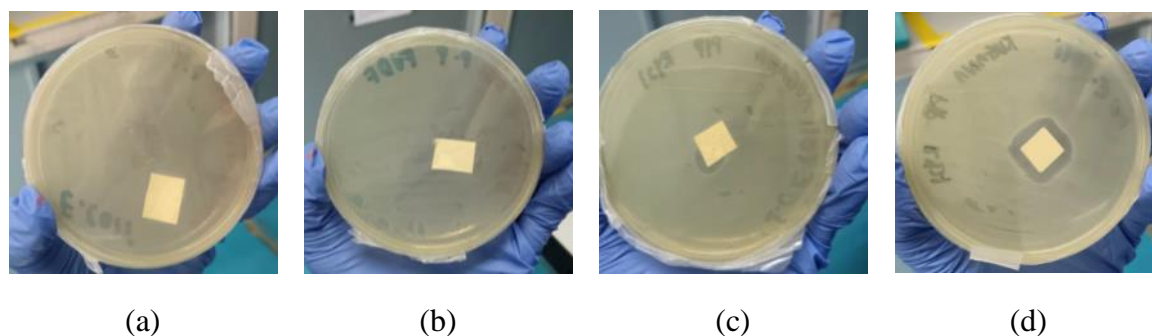


**Figure 3.** The inhibition zone formed on (a) Pure PVDF, (b) 0.1 g chitosan/PVDF, (c) 1.0 g chitosan/PVDF, and (d) 2.0 g chitosan/PVDF membranes.

From Figure 3, it can be observed that there is no inhibition zone around the pure PVDF membrane. This shows that the membrane is not resistant to microbes. This is due to the PVDF's hydrophobic nature makes it easier for it to interact with organic molecules, causing fouling on the membrane surfaces and shortening the membranes' lifespan (Pramono *et al.*, 2023).

For the chitosan/PVDF membranes, the inhibition zone differs for different concentrations of chitosan used. The 0.1 g chitosan/PVDF membrane showed no inhibition zone, which proves that the membrane was also not resistant to the microbes. This might be because the concentration of chitosan mixed with PVDF was not sufficient to create a strong antibacterial resistance. Below a certain concentration, the chitosan may not reach the level required to effectively disrupt the bacterial cells or interfere with their growth (Asadi *et al.*, 2022). On the other hand, the 1.0 g and 2.0g chitosan/PVDF membranes showed some positive results. The inhibition zone of the 2.0 g chitosan/PVDF membrane was the largest compared to the other membranes. It can be observed that the membrane exhibited antimicrobial properties. Although several different mechanisms have been hypothesised, the precise mechanism behind chitosan's antibacterial action remains unclear. The binding of the negatively charged fluoride atoms to the cationic amine group in chitosan is one of the most often proposed methods. This binding interferes with regular cellular activity and modifies the permeability of the membrane (Mirbagheri *et al.*, 2023). In conclusion, the concentration of the chitosan must reach a certain level that can allow the chitosan particles to exhibit antibacterial protection to the PVDF membrane.

#### 4. Conclusions

The 2.0 g chitosan/PVDF membrane exhibited positive results for all characterisations. Firstly, the membrane showed the lowest contact angle and the highest percentage of porosity compared to the other membranes. Then, the membrane showed the

largest inhibition zone during the Halo–zone test. This proved that the 2.0 g chitosan/PVDF membrane was antifouling resistant and has antimicrobial protection, which can prevent any bacterial contamination from accumulating on the surface of the membrane.

**Author Contributions:** Kuganagiesry Subramaniam, Ain Nur Nadhira Shurizan, and Nur Suhaili Mohd Yatim conducted the literature search, analyzed the included studies, and wrote the entire manuscript.

**Funding:** Funding by the Ministry of Higher Education Malaysia under the Fundamental Research Grant Scheme (FRGS/1/2020/TK0/UNIMAP/02/103), University Malaysia Perlis.

**Acknowledgements:** The authors acknowledge the financial assistance and facilities provided by the Ministry of Higher Education Malaysia under the Fundamental Research Grant Scheme (FRGS/1/2020/TK0/UNIMAP/02/103), University Malaysia Perlis.

**Conflicts of Interest:** The authors declare no conflict of interest.

## References

- Abriyanto, H. (2021). Hydrophilic Modification of PVDF Membrane: a Review. *Journal of Membranes and Materials*, 1(1), 1–9. Retrieved from <https://ejournal2.undip.ac.id/index.php/jmm/article/view/10516>
- Ali, A., Zhang, N., & Santos, R. M. (2023). Mineral Characterization Using Scanning Electron Microscopy (SEM): A Review of the Fundamentals, Advancements, and Research Directions. *Applied Sciences*, 13(23), 12600. <https://doi.org/10.3390/app132312600>
- Asadi, A., Gholami, F., Nazari, S., *et al.* (2022). Preparation of antifouling and antibacterial polyvinylidene fluoride membrane by incorporating functionalized multiwalled carbon nanotubes. *Journal of Water Process Engineering*, 49, 103042. <https://doi.org/10.1016/j.jwpe.2022.103042>
- De Santa Catarina, U. F., Machado, R. a. F., & Hotza, D. (2022). Porous chitosan membranes with high porosity shaped by solvent evaporation technique in water as a solvent and acetone as a non-solvent. <https://repositorio.ufsc.br/handle/123456789/236184>
- Pasieczna-Patkowska, S., Cichy, M., & Flieger, J. (2025). Application of Fourier Transform Infrared (FTIR) Spectroscopy in Characterization of Green Synthesized Nanoparticles. *Molecules*, 30(3), 684. <https://doi.org/10.3390/molecules30030684>
- Jiang, W., Lee, S., Zan, G., *et al.* (2023). Alternating current electroluminescence for Human-Interactive sensing displays. *Advanced Materials*, 36(8). <https://doi.org/10.1002/adma.202304053>
- Kumari, S., & Kishor, R. (2020). Chitin and Chitosan: origin, properties, and applications. In *Elsevier eBooks* (pp. 1–33). <https://doi.org/10.1016/b978-0-12-817970-3.00001-8>
- Mirbagheri, V. S., Alishahi, A., Ahmadian, G., *et al.* (2023). Toward understanding the antibacterial mechanism of chitosan: Experimental approach and in silico analysis. *Food Hydrocolloids*, 147, 109382. <https://doi.org/10.1016/j.foodhyd.2023.109382>
- Pramono, E., Umam, K., Sagita, F., *et al.* (2023). The enhancement of dye filtration performance and antifouling properties in amino-functionalized bentonite/polyvinylidene fluoride mixed matrix membranes. *Heliyon*, 9(1), e12823. <https://doi.org/10.1016/j.heliyon.2023.e12823>

Purkait, M. K., Sinha, M. K., Mondal, P., *et al.* (2018). Introduction to membranes. In *Interface science and technology* (pp. 1–37). <https://doi.org/10.1016/b978-0-12-813961-5.00001-2>

Xie, Q., Zhang, S., Hong, Z., *et al.* (2018). Effects of casting solvents on the morphologies, properties, and performance of polysulfone support and the resultant graphene oxide-embedded thin-film nanocomposite nanofiltration membranes. *Industrial & Engineering Chemistry Research*, 57(48), 16464–16475. <https://doi.org/10.1021/acs.iecr.8b04515>



Copyright © 2026 by Subramaniam, K, *et al.* and HH Publisher. This work is licensed under the Creative Commons Attribution-NonCommercial 4.0 International License (CC-BY-NC4.0)